Microbial Ecology

Development and Structure of Eukaryotic Biofilms in an Extreme Acidic Environment, Río Tinto (SW, Spain)

Angeles Aguilera[1], Virginia Souza-Egipsy[1], Felipe Gómez[1] and Ricardo Amils[1,2]

(1) Centro de Astrobiología, Instituto Nacional de Técnica Aeroespacial, Carretera de Ajalvir Km 4, 28850 Torrejón de Ardoz, Madrid, Spain
(2) Centro de Biología Molecular (UAM-CSIC), Universidad Autónoma de Madrid, Canto Blanco, 28049, Madrid, Spain

Received: 6 February 2006 / Accepted: 8 April 2006 / Online publication: 1 February 2007

Abstract

An *in situ* colonization assay was performed to study the early stages of biofilm formation in Río Tinto (SW, Spain), an extremely acidic environment (pH ca. 2). Eukaryotic assemblages were monitored at monthly intervals for 1 year. Diversity, colonization rates, and seasonal variations were analyzed. Structural features of naturally grown biofilms were explored by light and scanning electron microscopy in backscattered electron mode. A total of 14 taxa were recognized as constituents of the eukaryotic assemblages. The eukaryotic communities were dissimilar at the different sampling sites. The lowest diversity was found at the most extreme locations, in terms of pH and heavy metal concentrations. The biofilms were mainly formed by species from the genera *Dunaliella* and *Cyanidium*. Two genera of filamentous algae, *Zygnemopsis* and *Klebsormidium,* were principally responsible for the variability in the cell number throughout the year. These species appear in June to decrease almost completely between October and November. In contrast, the number of heterotrophic flagellates and ciliates remained constant throughout the year. The microcolonization sequence showed an initial accumulation of amorphous particles composed of bacteria and inorganic grains of minerals. By the end of the second month, the organic matrix was also populated by fungi, bacteria, and a few eukaryotic heterotrophs such as amoebae and small flagellates. Diatoms only showed significant colonization in regions where mycelial matrices were first established. Flagellated green algae such as *Dunaliella* or *Chlamydomonas* as well as *Euglena* were also present at the very beginning of the biofilm development, although in low numbers (<100 cells cm^{-2}). After the flagellated cells, sessile species of algae such *Chlorella* or *Cyanidium* appeared. Filamentous algae were the last species to colonize the biofilms. Most of the naturally grown biofilms were found to be structures composed of different species organized in different layers separated, probably by extracellular polymeric substances, although more analysis should be done in this regard. The possible implications of the biofilm structure in the adaptation to this extreme habitat are discussed.

Correspondence to: Angeles Aguilera; E-mail: aaguilera@cbm.uam.es

Introduction

Río Tinto (SW, Spain) flows through the Iberian Pyritic Belt, one of the richest metal sulfide ore deposits on Earth [8]. These ores have been mined for centuries since the 3rd millennium B.C., making it one of the oldest mining areas known [18]. Río Tinto originates in this mining area and flows ca. 90 km into the Atlantic Ocean. The river has a constant low pH (range 0.8 to 3; mean 2.3), buffered by ferric iron and with high concentrations of dissolved heavy metals, reaching 20 g l^{-1} of Fe [33]. The unusual water physicochemical characteristics convert the river into one of the largest acidic environments studied to date.

The extreme conditions of the river are the product of the metabolic activity of chemolithotrophic microorganisms, mostly iron- and sulfur-oxidizing bacteria that can be found in high concentrations in its waters. Their iron-oxidizing metabolism is responsible for the solubilization of sulfidic minerals (mainly FeS_2) and the correspondent high concentration of ferric iron, sulfate, and protons in the water column [19, 25]. The result is a strong acidic solution of ferric iron that brings into the solution other cationic metals, including high concentration of heavy metals. Most of these chemolithotrophic prokaryotes are autotrophic, and thus, in addition to promoting the extreme conditions of the habitat, they are also primary producers [25, 33].

 DOI: 10.1007/s00248-006-9092-2 • Volume 53, 294–305 (2007)

However, what makes the Tinto river a unique acidophilic extreme environment is that eukaryotic organisms are the principal contributors of biomass in the river; over 65% of the total biomass is attributable to a remarkable degree of eukaryotic diversity found in its waters [1, 33, 34]. Members of the Bacillariophyta, Chlorophyta, and Euglenophyta phyla as well as ciliates, cercomonads, amoebae, stramenopiles, fungi, and yeast have been detected [1, 33, 34]. Most of the eukaryotic microbial communities found in the river are distributed in extensive biofilms along the riverbed. As in other habitats, monospecies biofilms are relatively rare and thus most biofilms are composed of mixtures of microorganisms [50]. The macroscopic shape and species composition of the biofilms vary greatly throughout the river. Some of them adopt filamentous morphologies in flowing water, whereas others form thick, colorful patches firmly attached to the mineral substrates.

Bacterial biofilms are organized multicellular systems with a structural and functional architecture that influences metabolic processes, response to nutrients, predation, and other factors of the ecosystem [13]. Consequently, structural studies of microbial biofilms and their formation play a critical role in understanding the ecophysiological processes in natural habitats. Moreover, it is important to study how biofilms in highly acidic conditions affect geochemical processes as metal immobilization [30, 46, 48] and influence the ecophysiological rates of the microorganisms [12, 40] when compared to microorganisms growing in a planktonic form [35, 39]. This is even more important in extreme environments where forming a structured biofilm might protect the organisms from external stress conditions and allow them to resist more extreme conditions [41].

Knowledge of biofilm structure and function has grown significantly in the last few years because of advances in microscopical techniques from laser scanning confocal [31] to cryoscanning microscopy [44]. However, most of these studies were performed on bacterial biofilms and very few studies have explored the structural features of eukaryotic biofilms. Although previous studies have focused on the analysis of the genetic diversity of eukaryotic organisms in Río Tinto [1, 32–34], this study focuses on the description of the arrangement and organization between the different species in time and space. The objective of this study was to analyze the architecture, seasonal variation, and colonization processes of several eukaryotic biofilms during seasonal variations. Because the dynamics of the river, which are related to seasonal variations in the flow and stability of the riverbed sediments, make the sampling of biofilms grown on the original substrate very difficult, we studied seasonal variation and colonization rates on glass plates distributed along the river. In addition, the structural features of naturally grown biofilms were also analyzed by light and scanning electron microscopy in backscattered electron (SEM-BSE) mode by using a preparation technique that has been described as an *in situ* approach for the study of microbial communities [18].

Methods

Study site and sampling locations. Río Tinto, located in SW Spain, can be divided into three main zones—the origin, the transitional, and the estuary—based on topological, geological, and geochemical characteristics [17, 19]. The origin of the river is characterized by its extreme physicochemical conditions in terms of low pH, with an annual mean value of 2.2, and high concentrations of heavy metals in comparison to those found in nearby rivers [32, 33].

A general description of Río Tinto physicochemical parameters as well as geological records and hydrochemistry conditions has already been provided [19, 33]. Seasonal variations in geochemical conditions result from alternating wet and dry seasons, during the winter and summer months, respectively. January rainfalls exceeding 120 mm are common, contrasting with the little or no rainfall observed from July through September.

Biofilms were studied at seven different locations along the course of the river (Fig. 1). (1) FE, nominally considered the "origin" of the river, is a very red stream formed by water coming from three adjacent streams. (2) AG, a small surface stream formed by combination with water seeping out of a bank, has some of the most conspicuous biofilms of the river. (3) ANG is a spring emerging from a pile of loose rocks; here, the water temperature is elevated (ca. 25°C year round). (4) RI, located at the exit of a small tunnel, has the lowest pH (ca. 1.1 year round) and the highest amounts of heavy metals. (5) NU also springs from a pile of rocks. (6) UMA is a small stream with moderate water flow that joins the river downstream from the origin. (7) CEM is located about 10 km downstream from the origin where the river widens.

The sampling sites in this study were selected by taking into account previous analysis of the physicochemical characteristics of the water [19, 25, 32, 33]. From the seven sites selected, RI and UMA showed the most extreme parameters in terms of pH (ca. 1.1 year round) and heavy metals, with 20 g L^{-1} of Fe or 130 mg L^{-1} of Cu [20]. ANG and FE followed closely with a pH of ca. 1.5 the whole year round and 15 g L^{-1} of Fe or 4.8 g L^{-1} of Al. The remaining locations (AG, NUR, and CEM) showed milder physicochemical water parameters, pH ca. 2.0, as well as lower amounts of heavy metals.

Sampling device and sampling procedure. To study seasonal dynamic and colonization processes, a

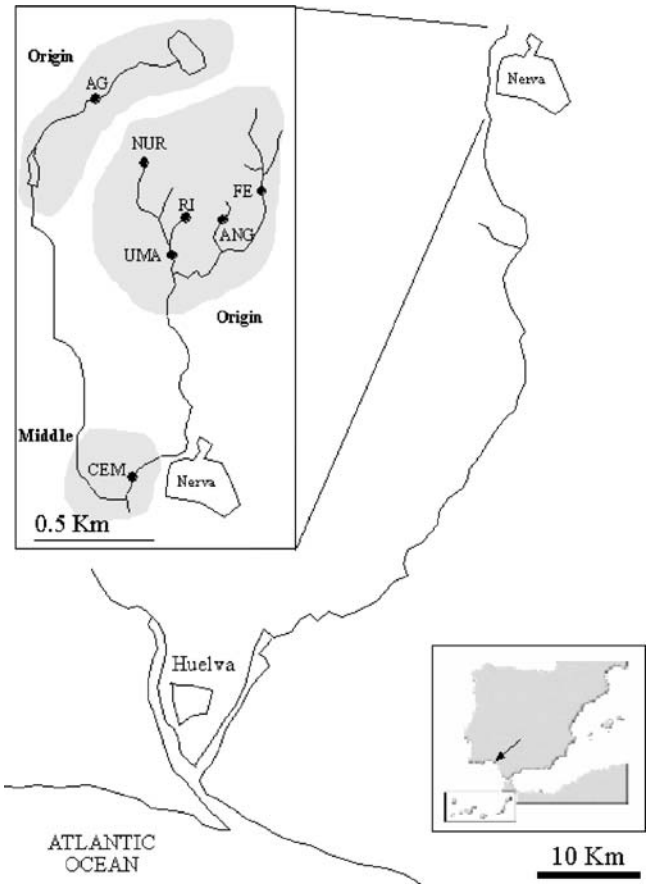

Figure 1. Schematic map of Río Tinto in which sampling stations are indicated. *Insert:* a detailed map of the origin area.

biofilm collector was constructed. This device consisted of a wood frame carrying 12 glass microscopic slides. Two frames per sampling location were placed below the river surface by using weights and perpendicularly to the water current flow. Biofilms were harvested monthly after their placement, from January 2003 until January 2004. Every 30 ± 5 days, one glass slide from each frame was taken out at random, protected with a sealed coverslip (SecureSeal slides, Grace BioLabs, Germany), and transported to the laboratory on ice. The cell counts were carried out within the same day, by using a microscopic counting grid (156.25 mm^2) coupled to the 10× eyepiece of a Zeiss Axioscope II equipped with phase contrast. For each sample, ca. 50 randomly chosen microscopic fields were counted at 400-fold magnification. For unicellular organisms, cell numbers were counted as well as for filamentous organisms, because their total length usually exceeds the total length of the slide. In all cases, cell counts were expressed as the number of cells counted on 1 cm^2 of slide surface.

At the same time, the percentage of the surface covered by eukaryotic cells was calculated by using the public domain ImageJ program (National Institutes of Health, Bethesda, MD, USA; http://rsb.info.nih.gov/ij/). Images of the biofilms were captured with a CCD camera coupled to the microscope with no compression in order to preserve pixel data.

Identification of algae and heterotrophic protists were carried out by direct microscopic observation using different phenotypic features based on previous studies of the eukaryotic diversity founded in this river [1, 33].

Scanning electron microscopy in backscatterred electron mode SEM-BSE. We collected natural substrate grown biofilms in September 2004 to study their structure by using SEM. At least two small pieces (2–3 cm^2) of characteristic biofilms in each locality growing on the natural host material were placed in 6 multiwell plates (Corning, NY, USA). The flow direction was recorded and kept through all the processing. The selection of the biofilms was carried out based on previous studies regarding their species composition. The biofilms were secured for transport with a thin layer of alginic acid (1%), which gelled in place on the biofilm surface after the addition of $CaCl_2$ (1%). Samples were fixed in 2.5% glutaraldehyde in 1 mM HEPES buffer (pH 7). The samples were kept cold (5°C) and in the dark until further processing. In the laboratory, samples were washed with HEPES buffer and postfixed with 1% osmium tetroxide in distilled water for a minimum of 8 h. Samples were dehydrated by using an ascending series of ethanol and then infiltrated with LR-White resin for 24 h. The infiltrated samples were polymerized at 65°C for 24 h. Once polymerized, the blocks were cut transversally with a diamond saw, fine-polished and carbon-coated following previous protocols [2, 49], and examined under a scanning electron microscope with backscattered electron detection (BSE). Transverse sections of the polished surfaces of the rocks were examined via a JEOL 5600LV SEM equipped with a BSE detector.

Statistical analysis. Because of heterogeneous variances in microbial parameters, Kruskal–Wallis nonparametric tests were used to analyze differences between stations and sampling dates [43]. A 5% significance level ($p < 0.05$) was used for rejection of null hypothesis in all cases.

Results

Eukaryotic community structure and seasonal variation. A total of 14 taxa were recognized as constituents of the eukaryotic assemblages in the artificial substrate biofilms. Epifluorescence and phase contrast microscopy allowed the identification of 18 species belonging to different genera: *Pinnularia* (Bacillariophyta), *Euglena* (Euglenophyta), *Cyanidium* (Rodophyta), three genera of Chlorophytas (*Chlamydomonas*, *Chlorella*, and

Dunaliella), two genera of filamentous algae, *Zygnemopsis* and *Klebsormidium* (Streptophyta), two species of amoebae from the genera (*Vahlkampfia* and *Naegleria*), one species of heliozoan belonging to the genera (*Actinophrys*), four species of flagellates from the genera (*Bodo*, *Cercomonas*, *Ochroomonas*, and *Labirynthula*), two genera of ciliates (*Oxytrichia* and *Colpidium*), and one species of rotifer that belongs to the genera (*Rotaria*). Chlorophytas and *Euglena* comprised nearly 80% of the benthic community during study. In the same manner,

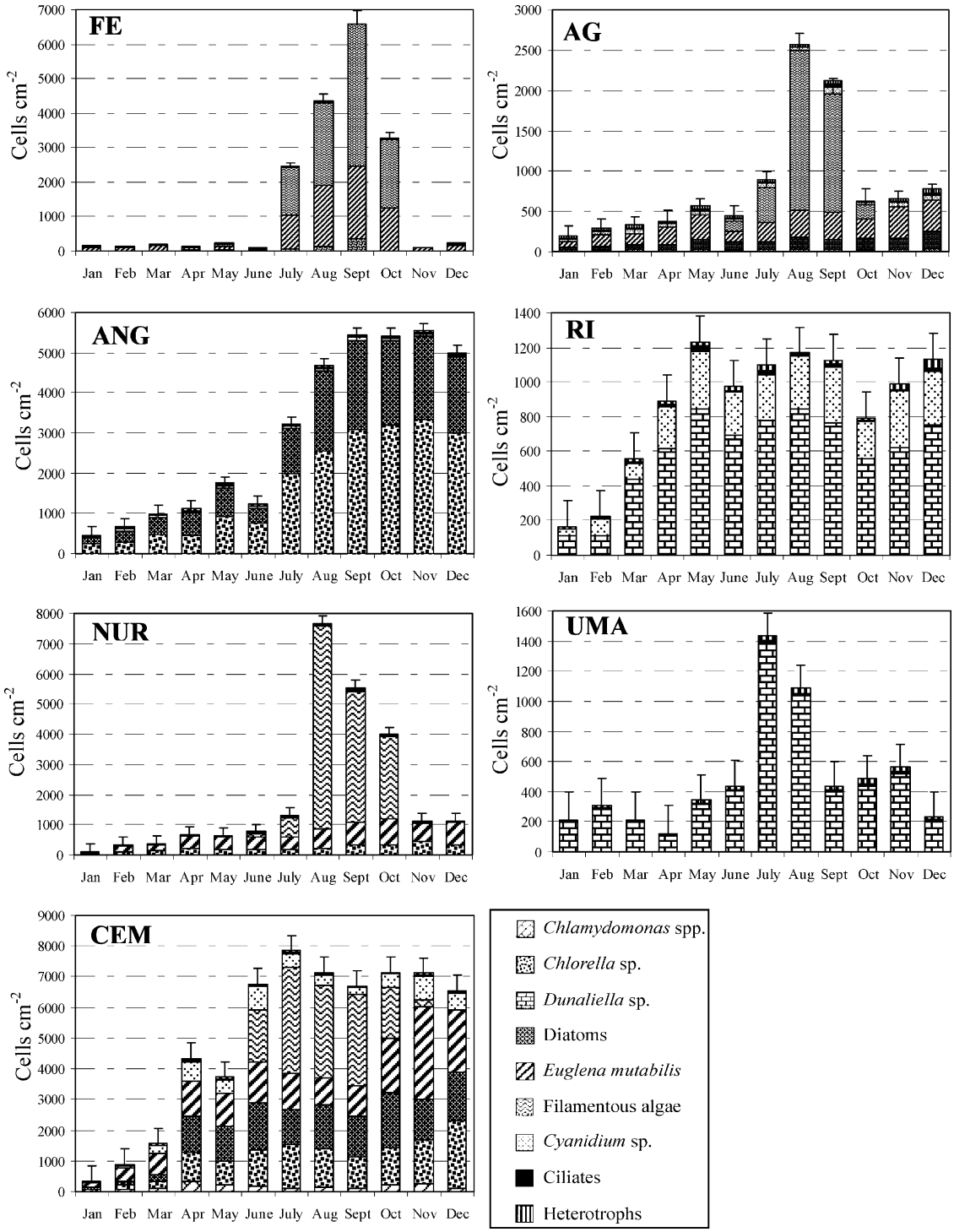

Figure 2. Abundance of major phylogenetic groups in artificial river biofilms during one annual cycle determined by microscopy. Filamentous algae (*Zygnemopsis* and *Klebsormidium*), Ciliates (*Oxytrichia*), Heterotrophs: amoebae (*Vahlkampfia*), heliozoa (*Actinophrys*), flagellates (*Bodo*, *Cercomonas*, *Ochroomona*, *Labirynthula*), and rotifers (*Rotaria*).

viable bacteria and fungi were present in all the samples analyzed.

Direct microscopic counts were used to estimate total species abundances at each site (Fig. 2). In general, there were significant differences in total cell numbers among sampling locations and sampling dates ($p < 0.05$). Cell densities were significantly lower ($p < 0.05$) on RI and UMA, two of the most extreme sampling sites found in the river. Mean densities associated with these sites were 861 ± 321 and 496 ± 298 cells cm^{-2}, respectively, compared to 5009 ± 1231 for CEM, the sampling site with the highest cell density.

Two different patterns of colonization were observed. At FE, AG, NU, and UMA, cell abundance was significantly higher in summer than in winter ($p < 0.05$), showing considerable seasonality. However, at ANG, RI, and CEM, the number of cells increased progressively from January to late spring, and remained constant the rest of the year.

The eukaryotic community found in the biofilms was quite dissimilar at the different sampling sites (Fig. 2). The lowest diversity was also found in RI and UMA, the most extreme locations, where biofilms were mainly formed by *Dunaliella* cells and *Cyanidium*. No significant differences were found in their eukaryotic assemblages during the year ($p > 0.05$). On the other hand, CEM was the most diverse site, showing species from all the taxa identified.

Filamentous algae (*Zygnemopsis* and *Klebsormidium*) were mainly responsible for the variability in cell number throughout the year, as we can see for FE, ANG, or NU. These species appeared in June, to disappear almost completely between October and November. In contrast, heterotrophic flagellates and ciliates remained significantly constant throughout the year in all the sampling sites analyzed ($p > 0.05$).

Colonization rates. For most of the sampling sites analyzed, 1 month after the slides were placed in the river, 50–70% of the surface was coated with a thin film of amorphous particles composed of both aggregated organic matter formed mainly by bacteria as well as inorganic grains of minerals (Fig. 3). It was apparent that by the end of 2 months the organic matrix was also populated by fungi, bacteria, and few eukaryotic heterotrophs such as amoebae and small flagellates belonging to the genera *Bodo* and *Cercomonas*. At this point, the aggregated organic/inorganic matter was sufficiently dense to mask any significant influence of the underlying glass surface, with more than 90% of the surface covered. Furthermore, it was noticeable that diatoms only showed significant colonization in those regions where mycelial matrices were established first. Flagellated green algae such as *Dunaliella* or *Chlamydomonas* as well as *Euglena* were also present from the very beginning of the biofilm development, although in low number. Sessile species of algae such as *Chlorella* or *Cyanidium* followed the flagellated cells and were present in significant amounts. Filamentous algae were the last species to colonize the biofilms. Only two locations, RI and UMA showed coverage values lower that 50%, and it took more than 6 months to reach these percentages.

Once the biofilm was formed, the percentages of coverage remained constant throughout the year for all studied locations, except for FE located at the origin of the river, where the coverage decreased during winter ($p < 0.05$).

Eukaryotic community structure in naturally grown biofilms. SEM-BSE images of natural grown biofilms are summarized in Figs. 4–7. All selected biofilms were macroscopically clearly different from each other and can be considered representative of the biofilms in the area where they were collected. The biofilm from FE (Figs. 4A, B) showed two clearly different layers. The upper one was formed by *Euglena* and the lower layer had the diatom *Pinnularia* as the dominant species. The separation between layers is attributable to the presence of an area with a lower number of cells and probably more extracellular polymeric substance (EPS). The diatom area is in contact with the substrate and it also has layers of minerals (Fig. 4A, arrows). The ultrastructure of the *Euglena*

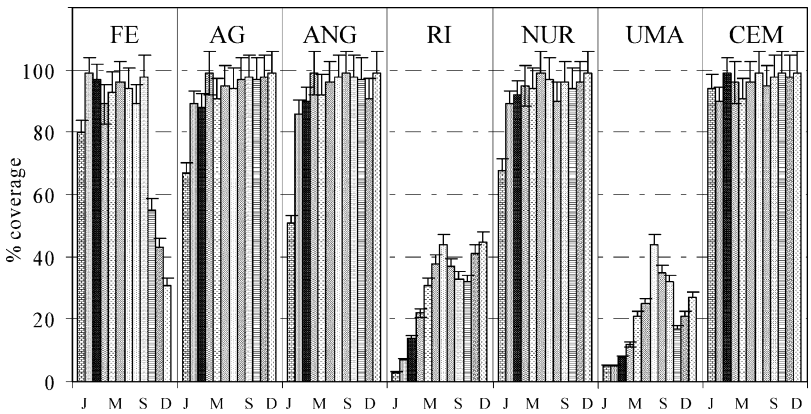

Figure 3. Percentage of surface coverage in artificial river biofilms during one annual cycle. Error bars represent standard deviation.

cells is clearly observed in the upper part of the biofilm (Fig. 4A). There were no minerals between the cells.

The biofilms observed in RI were some of the thinnest found in the river and mainly composed of *Dunaliella* (Figs. 4C, D). *Dunaliella* cells overlay a layer of loose mineral material above the substrate and some protists, such as amoebas, were also embedded in the biofilm (Fig. 4C, arrows). The two different layers could also be observed to be separated by EPS. A detailed view of the biofilm indicated that the lower layer was formed by *Dunaliella* cells, overlaying a layer of fine minerals and filamentous fungi (Fig. 4D, arrows).

Figure 5 summarizes the images obtained from naturally grown biofilms sampled at AG. Microscope observations revealed the lack of cell stratification and also showed that the biofilms were interbedded with layers of minerals (Fig. 5A). Cells were densely packed and the layers were not clearly differentiated (Fig. 5B). Field observations revealed that these biofilms were the thickest ones found in the river because of their loose structure. Although up to six eukaryotic species were found, only three were the dominant taxonomic groups: diatoms, *Chlorella*, and *Chlamydomonas* (Fig. 5C). Cells on the upper part of the biofilm had empty interior and bright cell walls (Fig. 5C, arrows) indicative of decay and precipitation of minerals around the external surface of the cells [18]. Toward the upper part of the biofilm, the intercellular spaces were filled with iron oxides (Fig. 5D)

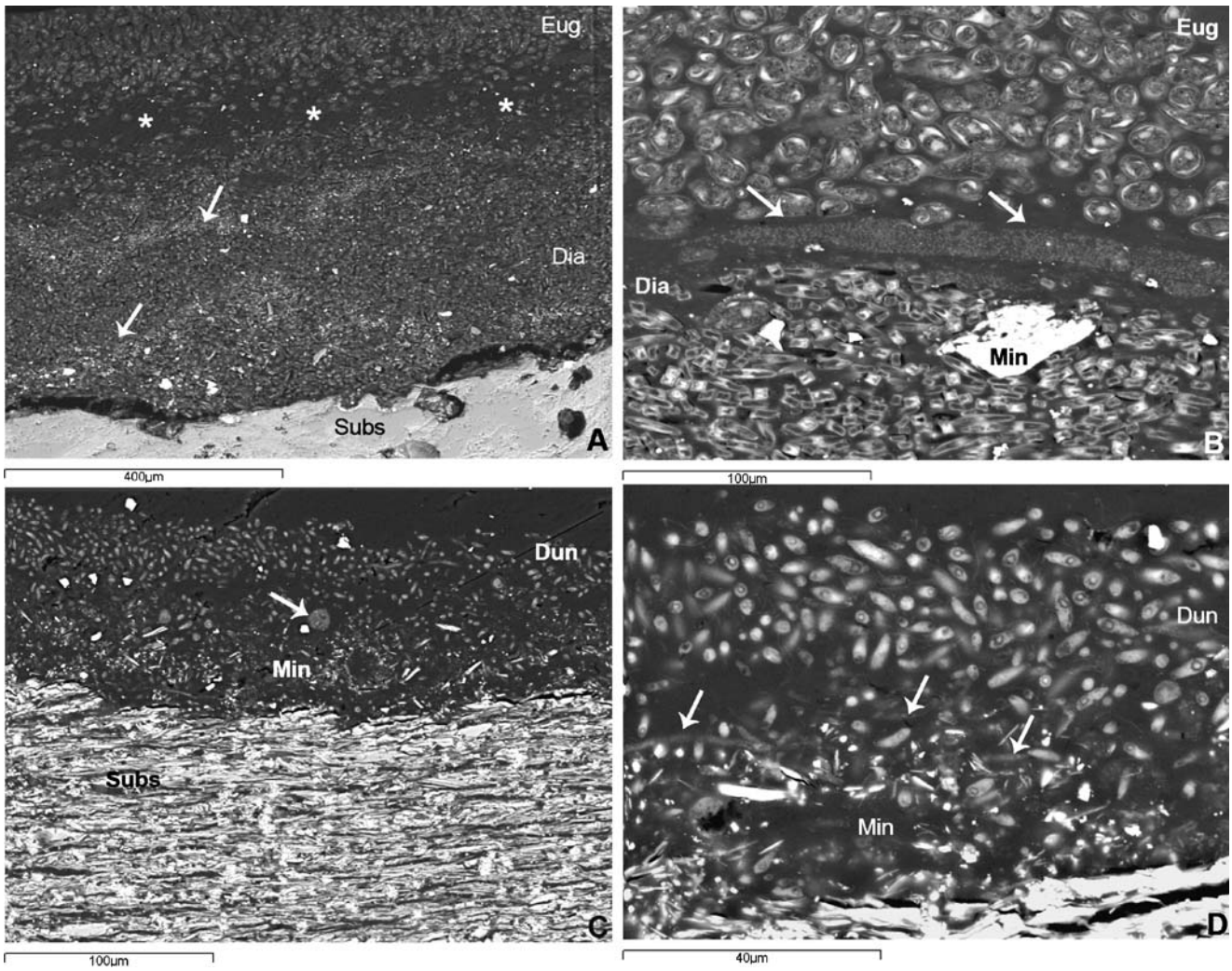

Figure 4. SEM-BSE images of natural grown biofilms from FE (A and B) and RI (C and D). (A) General view of FE biofilm formed by a combination of *Euglena* (Eug) and diatoms (Dia). The separation between layers is attributable to EPS (*asterisks*). The diatom area is in contact with the substrate (Subs) and layers of minerals are also shown (*arrows*). (B) Transversely sectioned *Euglena* cells located at the upper part of the biofilm, whereas diatoms (Dia) are accumulated at the bottom. Both layers were separated by EPS (*arrows*). The diatom biofilm have some minerals present in between the cells (Min). (C) General view of biofilms from RI. The *Dunaliella* (Dun) cells overlay a layer of loose mineral material (Min) above the substrate (Subs). Some protists are also embedded in the biofilm (*arrow*). (D) *Dunaliella* cells (Dun) surrounded by small mineral particles (Min) and fungi (*arrows*).

and some cells also have minerals inside the space delimited by the cell walls (Fig. 5D, arrows).

Biofilms from ANG showed a completely different vertical assemblage (Fig. 6). In this part of the river, biofilms were mainly produced by diatoms and *Chlorella*, forming a patched distribution on the pebbles. As in most of the other biofilms, two different layers could be observed (Fig. 6A). Usually, the diatoms widely dominated the upper part of the biofilms, being densely packed with almost a vertical orientation. The bottom layer was composed of *Chlorella* cells. The two layers were separated by a film with less cells and probably filled with EPS (Fig. 6A, asterisks). Some protists such as amoebas were also present in the biofilm (Fig. 6A, arrows). In some areas of the biofilms, the upper part was colonized by *Chlorella*, showing a separation from the diatoms by an area with less cells and filled with EPS (Fig. 6B, asterisks). The bottom layer is also characterized by the presence of bacteria between the cells (Figs. 6C, D).

Images obtained from biofilms collected at CEM are shown in Fig. 7. Field observations showed also that these biofilms were the thickest ones studied after the ones found in AG; in this case, however, the consistency of the biofilms was more compact. The general structure of the biofilms found at CEM had a peculiar distribution of spherical inclusions instead forming the usual layers (Fig. 7A, asterisks). A detailed image of the upper part of the biofilm showed that it was formed almost exclusively

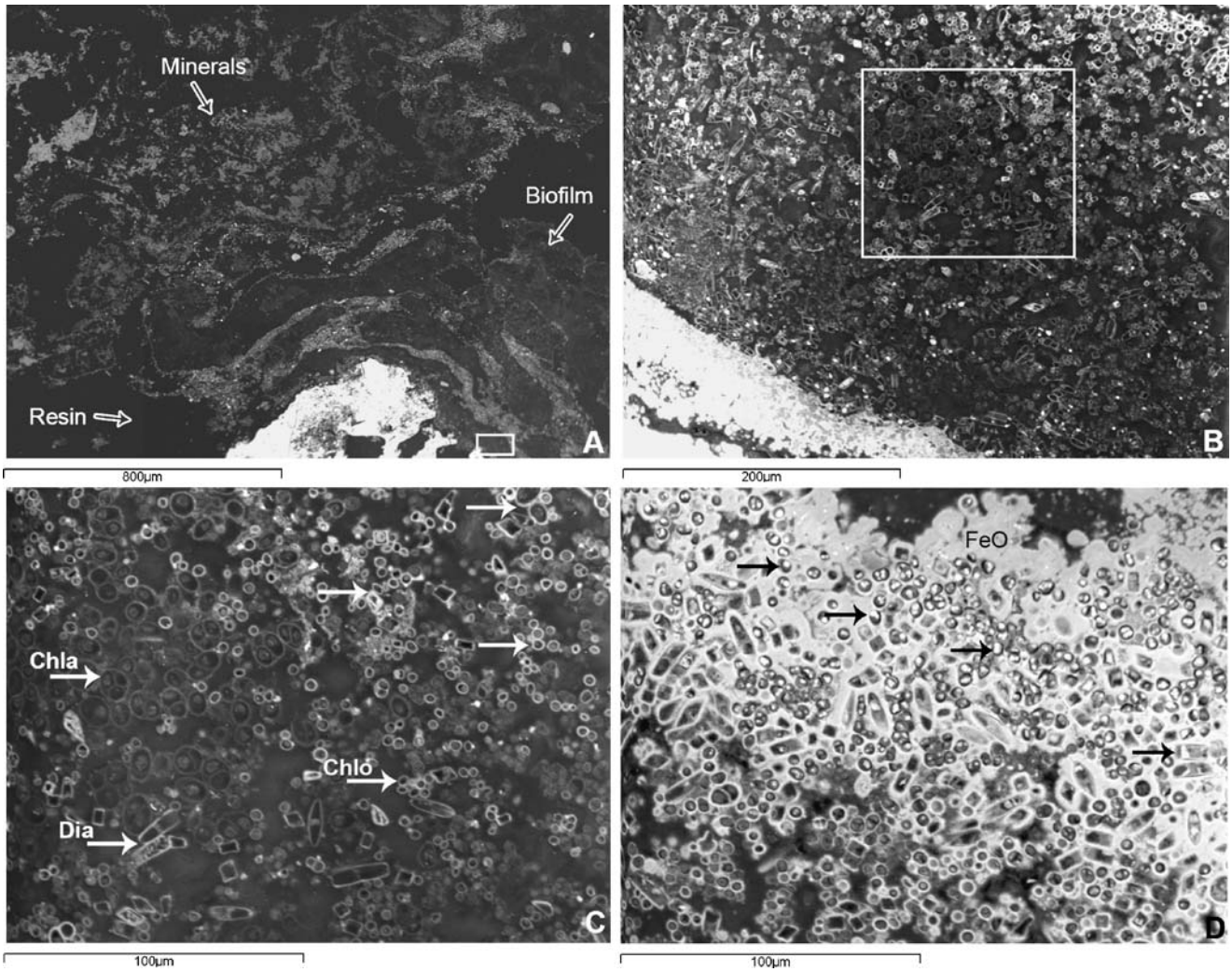

Figure 5. SEM-BSE images of natural grown biofilms from AG. (A) Biofilms are interbedding with layers of minerals. The black areas in the images are filled with resin. (B) Detailed view of the square in (A) showing biofilms between layers of minerals. The cells are densely packed and there is not a clear differentiation in layers. (C) Detailed view from the square in (B), showing the species composition, diatoms (Dia), *Chlorella* (Chlo), and *Chlamydomonas* (Chla).Cells on the upper part of the biofilm show an empty interior and brighter cell walls (*arrows*), indicative of decaying and precipitation of minerals around the external surface of the cells. (D) Towards the upper part of the biofilm the intercellular spaces in the biofilm became filled with iron oxides (FeO) and some cells have also minerals inside the space delimited by the cell walls (*arrows*).

by diatoms and colonies of bacteria (Fig. 7B). Some minerals were also present between the cells. The spherical inclusion areas (Fig. 7C, asterisks) had irregular edges and are filled with a not-contrasted material, indicating the presence of some organic material also visualized by optical microscopy. The lower part of the biofilm was in contact with the substrate and it was formed by a mixture of *Cyanidium* cells, diatoms, and bacteria (Figs. 7C, D).

Discussion

Differences in the physicochemical characteristics of the water explain the species assemblages and colonization rates of the eukaryotic biofilms present in each location. The most extreme sites, RI and UMA, showed significantly lower amounts of total cell abundances, species diversity, and colonization rates than the rest. Only *Dunaliella* and *Cyanidium*, two of the most acidophilic eukaryotic organisms known, were able to grow in appreciable amounts at these locations. These results are in agreement with a widely held ecological tenet stating that increasing environmental extremity leads to a decrease in biodiversity within that environment [3, 22]. According to this concept, a reduction in the diversity and abundance within a given environment should be evident along gradients in which environmental parameters become extreme. Our results also agree with this

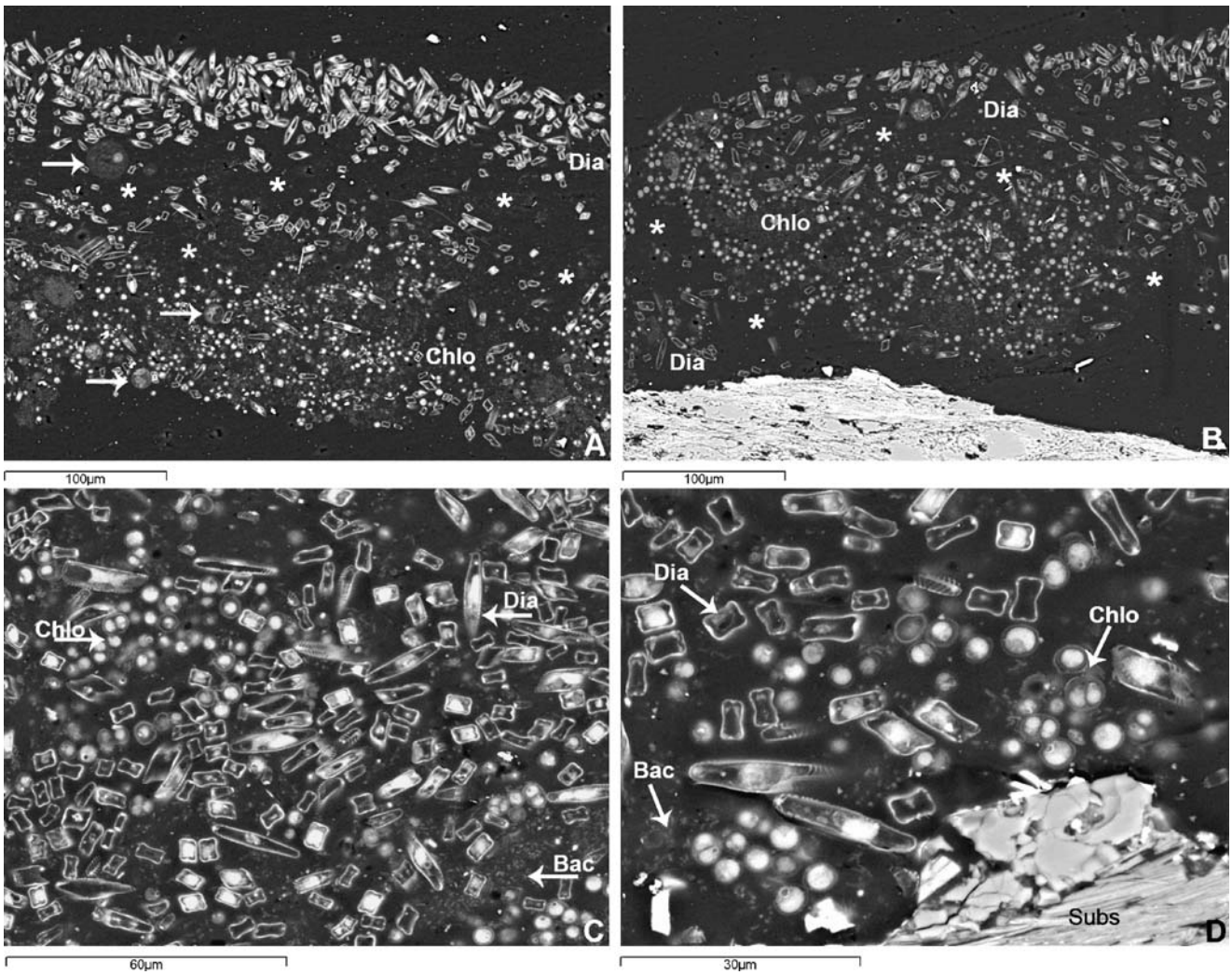

Figure 6. SEM-BSE images of natural grown biofilms from ANG. (A) Biofilms of diatoms (Dia) and *Chlorella* (Chlo) form a patched distribution on the pebbles. In some areas the diatoms are on the upper part, densely packed with a vertical orientation. The two biofilms are separated by a layer with less cells and probably filled with EPS (*asterisks*). Some protists are also present in the biofilm (*arrow*). (B) In some areas the upper part is accessible by *Chlorella* (Chlo). There is a separation of the diatoms (Dia) by an area with less cells most likely filled with EPS (*asterisks*). (C) Detail image of an area where both species form a mix biofilm (Chlo and Dia). Between the cells there are bacteria colonies (Bac). (D) A detailed view of the biofilm structure in the area in contact with the substrate (Subs). The biofilm is formed by a mix of diatoms (Dia), *Chlorella* (Chlo), and bacteria colonies (Bac).

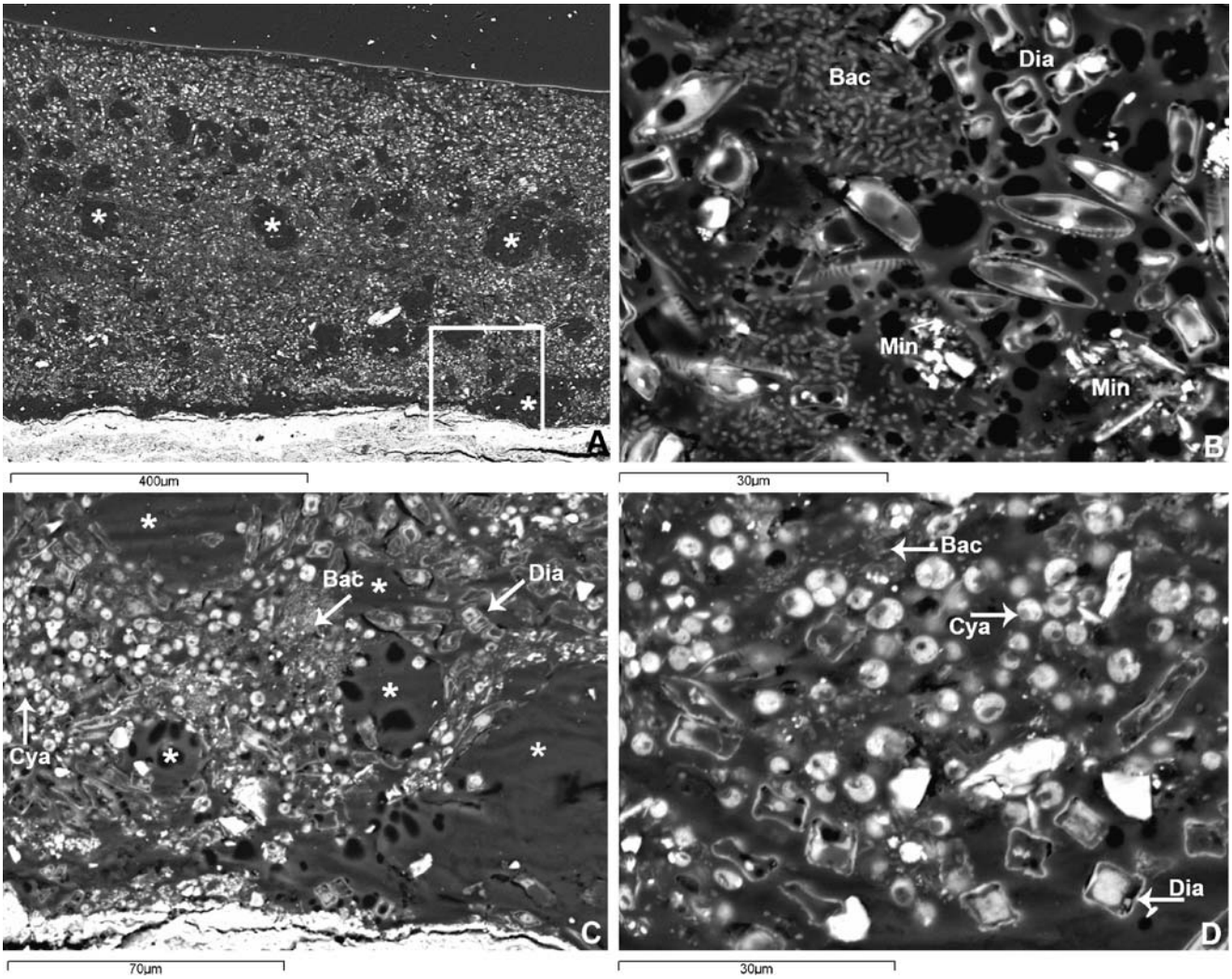

Figure 7. SEM-BSE images of natural grown biofilms from CEM. (A) These biofilms are the thickest ones studied. The general structure of the biofilms in CEM have a particular distribution of spherical inclusions (*asterisks*). (B) A detailed image of the upper part of the biofilm shows that is formed by diatoms (Dia) and colonies of bacteria (Bac). Some minerals are also present between the cells (Min). (C) Detailed image of the lower part of the biofilm in contact with substrate [square in panel (A)]. It is formed by *Cyanidium* cells (Cya), diatoms (Dia), and colonies of bacteria (Bac). The spherical inclusion areas (*asterisks*) have irregular edges indicating the presence of some organic material and not just air that will form perfect spherical bubbles. (D) The lower part of the biofilm is formed by a mixture of *Cyanidium* cells (Cya), diatoms (Dia), and bacteria (Bac).

statement. Thus, the highest eukaryotic biodiversity was found in CEM, which is located farthest from the origin and showing the least extreme water physicochemical parameters of all the analyzed sites [19, 20].

In the same regard, analysis of the annual cell density distribution denoted a clear bimodality for some of the sampling locations located at the very origin of the river (i.e., FE, AG, NUR, and UMA, Fig. 2). As during winter eukaryotic abundance was lower, this correlates with the bimodality in the annual water flow reported in previous studies on the Río Tinto area [19]. The climograms of this area showed a clear bimodality in the pluviosity and water current flow consisting of a humid and temperate season alternating with a warm and dry season. The high water table maintains the river flow during summer, although a high rate of evaporation induces higher concentrations of heavy metals as a result of concentration processes. This seasonal bimodality greatly influences the eukaryotic community biomass at these stations, where the slope is higher. In winter the water flow could be really fast (ca. 0.25 m s^{-1}) at these points, being able to remove most of the biofilms grown during summer. In this regard, the increase in eukaryote population in summer and late summer at these particular points is mainly attributable to two species of filamentous green algae (*Klebsormidium* and *Zygnemopsis*) being easier to remove via water flow. In general, green algae account for nearly all of the total eukaryotic biomass increase during

summer, which agrees with other studies conducted in extremely acidic environments [37, 38, 51]. This fact is closely related to the significant increase in temperature values and daylight as well as to the decrease in water flow—all of which facilitate cell deposition and biofilm formation.

The extensive permanent colonization by fungi and bacteria is the main reason for the unexpected lack of seasonality in the percentages of biofilm coverage despite seasonal changes in water flow and temperature. Our results show that the microbial colonization time sequence starts by the fixation of an organic conditioning biofilm formed mainly by fungal hyphae, bacterial and detrital mineral particles that will remain permanently attached to the substrate the whole time. The next step is colonization by pioneer motile eukaryotic species, such as amoeba or heterotrophic flagellates, followed by the establishment of an increasing number of sessile eukaryotes such *Chlorella* or diatoms. Finally, biofilm formation involves the incorporation of filamentous algae. A similar pattern of biofilm growth has previously been observed in other freshwater aquatic environments, and the nonspecific, permanent adhesion of bacteria and fungi to inert surfaces has been thoroughly described in past studies [14, 27, 47]. Thus, the development of this preconditioning substrata is of major importance to ensure colonization by autotrophs, especially in lotic systems [29].

The accumulation of periphyton biomass on the artificial surface used was much slower than the colonization rates reported in other studies, which stated that a 2- or 3-week colonization period was sufficient for the development of a mature community [6, 27]. Several factors may account for these differences. First is the choice of substratum, although several studies found no differences in periphyton growth and composition whether on glass slides, polyethylene, metals, cleaned stones and wood [6, 42]. Second, it could be due to a scarcity of available cells for colonization in the river. This fact is supported by our unpublished recent analysis of the water column where the water drifts typically contain less than 1000 cells L^{-1} of one of the major colonizer, *Euglena*. In the same manner, besides similarities regarding eukaryotic species composition, no further structural correspondences were found when artificial and natural biofilms from the same sampling location were compared.

In addition to biodiversity, microscale structural differences among naturally grown biofilms have also been observed in different localities. Although most of the biofilms from FE, RI, and ANG showed a unique, compact, and well-defined layered structure, biofilms sampled at AG showed several layers of cells loosely packed between layers of minerals. Different factors may be responsible for these structural differences. Several layers of sediment indicate fluctuations of the flow and rapid recolonization of the new surfaces. Several studies have demonstrated that age is a determining factor of biofilm structure, with the more loosely structured mats representing a younger state in biofilm development [26, 28]. In our case, most of the biofilms are significantly reduced every year during the rainy season. Differences in water velocity may also play a significant role in determining the biofilm structure [4, 5] and the amount of material accumulated on the sediments as in the sampling station CEM, allowing a higher density of material to accumulate. It has been demonstrated that some biofilm-forming microorganisms can produce sticky excretions that are able to trap allochthonous mineral particles within the mats in order to avoid being swept away by the current [23, 24].

Finally, intrinsic physiological features of the microorganisms forming the biofilm can be responsible for a specific structure. In biofilms, the matrix around the cells is a very important intrinsic factor related to physiology and environmental conditions. Some studies have reported that diatoms in marine habitats produce variable amounts of EPS under different environmental conditions [45]. In the case of bacteria, the complex regulation of surface attachment, surface binding, biofilm maturation, and—ultimately—biofilm detachment is affected by the physiology of the cells and by the physicochemical parameters of solid surfaces and environments [16]. However, in eukaryotic biofilms, data about intercellular regulation in the formation of biofilms are scarce.

Although other studies about microbial biofilms in acidic waters have been performed, most of them have focused on bacteria [7] or some groups of eukaryotic microorganisms such as diatoms or protozoans [9–11, 36]. Microbial biofilms at Río Tinto are tridimensional structures associated with surfaces that show a spectrum of structurally heterogeneous forms determined by the microorganisms and the environmental conditions. Our results highlighted the amount of information available about biofilm organization for study when using microscopy techniques that maintain the structure of the microbial communities [18]. However, this only marks the first step in understanding how intercellular association among the same species or different organisms could be a factor that allows the colonization of extreme acidic waters.

In conclusion, biofilm formation and structure reflected the adaptation of microorganisms to different environmental conditions on the upper part of the extreme acidic stream of Río Tinto. Periphytic algae, when forming biofilms with other microorganisms, might have nutritional advantages or specific microenvironmental conditions that allow them to be surrounded by substantially less severe physical and chemical conditions

than those of the external habitat [15, 21]. Further *in situ* microsensor techniques studies and controlled mesocosmos experiments will be necessary to fully understand the factors controlling biofilm formation and the association among different microorganisms.

Acknowledgments

The authors would like to thank Dr. S. Gonzalez for technical assistance in the colonization rates study. We are grateful to the Fundación Río Tinto for providing the facilities for completing this study in the field. Work by A.A. and V.S.-E. was supported by the Spanish Ministry of Education and Science through the program Ramón y Cajal. This work has been supported by grants to the Centro de Astrobiología at the Instituto National de Técnica Aeroespacial and CGL2005-05470/BOS grant.

References

1. Amaral, LA, Gómez, F, Zettler, E, Keenan, BG, Amils, R, Sogin, ML (2002) Eukaryotic diversity in Spain's river of fire. Nature 417: 137
2. Ascaso, C, Wierzchos, J (1994) Structural aspects of the lichen–rock interface using back-scattered electron imaging. Bot Acta 107: 251–256
3. Atlas, RM, Bartha, R (1997) Microbial Ecology: Fundamentals and Applications. Addison-Wesley Longman, Menlo Park, CA, USA, pp 336
4. Battin, TJ, Kaplan, LA, Newbold, JD, Cheng, X, Hansen, C (2003) Effects of current velocity on the nascent architecture of stream microbial biofilms. Appl Environ Microbiol 33: 5443–5452
5. Biggs, B, Close, M (1989) Periphyton biomass dynamics in gravel bed rivers: the relative effects of flows and nutrients. Freshw Biol 22: 209–231
6. Blinn, DW, Fredericksen, A, Korte, V (1980) Colonization rates and community structure of diatoms on three different rock substrata in a lotic system. Br Phycol J 15: 303–310
7. Bond, PL, Druschel, GK, Banfield, JF (2000) Comparison of acid mine drainage microbial communities in physically and geochemically distinct ecosystems. Appl Environ Microbiol 66: 4662–4671
8. Bourter, CA (1996) Did both extensional tectonics and magmas act as a major driver of convection cells during the formation of the Iberian Pyritic Belt massive sulfide deposits? J Geol Soc London 153: 181–184
9. Brake, SS, Dannelly, HK, Connors, KA, Hasiotis, ST (2001) Influence of water chemistry on the distribution of an acidophilic protozoan in an acid mine drainage system at the abandoned Green Valley coal mine, Indiana, USA. Appl Geochem 16: 1641–1652
10. Brake, SS, Dannelly, HK, Connors, KA (2001b) Controls on the nature and distribution of an alga in coal mine-waste environments and its potential impact on water quality. Environ Geol 40: 458–469
11. Brake, SS, Hasiotis, ST, Dannelly, HK (2004) Diatoms in acid mine drainage and their role in the formation of iron-rich stromatolites. Geomicrobiol J 21: 331–340
12. Camacho, A, Rochera, C, Silvestre, JJ, Vicente, E, Hahn, MW (2005) Spatial dominance and inorganic carbon assimilation by conspicuous autotrophic biofilms in a physical and chemical gradient of a cold sulfurous spring: the role of differential ecological strategies. Microb Ecol 50(2): 172–184
13. Costerton, JW, Cheng, KJ, Geesey, GG, Ladd, T, Nickel, JC, Dasgupta, M, Marrie, TJ (1987) Bacterial biofilms in nature and disease. Annu Rev Microbiol 45: 1921–1931
14. Corpe, WA (1980) Microbial surface components involved in adsorption of microorganisms onto surfaces. In: Bitton, G, Marshall, KC (Eds.) Adsorption of Microorganisms to Surfaces. Wiley, New York, pp 105–144
15. Davey, ME, O'Toole, GA (2000) Microbial biofilms: from ecology to molecular genetics. Microb Mol Biol Rev 64: 847–867
16. Davies, DG, Parsek, MR, Pearson, JP, Iglewski, BH, Costerton, JW, Greeberg, EP (1998) The involvement of cell-to-cell signals in the development of a bacterial biofilm. Science 280: 295–298
17. Davis, RA, Welty, AT, Borrego, J, Morales, A, Pendon, JG, Ryan, JG (2000) Rio Tinto estuary (Spain): 5000 years of pollution. Environ Geol 39(10): 1107–1116
18. De los Ríos, A, Ascaso, C, Wierzchos, J, Fernández-Valiente, E, Quesada, A (2004) Microstructural characterization of cyanobacterial mats from McMurdo Ice Shelf, Antarctica. Appl Environ Microbiol 70: 569–580
19. Fernández-Remolar, DC, Rodríguez, N, Gómez, F, Amils, R (2003) Geological record of an acidic environment driven by the iron hydrochemistry: the Tinto river system. J Geophys Res 108: 5080–5095
20. Fernández-Remolar, DC, Gómez-Elvira, J, Gómez, F, Sebastián, E, Martín, J, Manfredi, JA, Torres, J, González-Kesler, C, Amils, R (2004) The Tinto river, an extreme acidic environment under control of iron, as an analog of the *Terra Meridiani* hematite site of Mars. Planet Space Sci 52: 239–248
21. Flemming, HC (1993) Biofilms and environmental protection. Water Sci Technol 27: 1–10
22. Frontier, S (1985) Diversity and structure in aquatic ecosystems. Oceanogr Mar Biol 23: 253–312
23. Gerdes, G, Krumbein, WE (1987) Biolaminated deposits. In: Bhattacharya, S, Friedman, GS, Neugebauer, HJ, Seilacher, A (Eds.) Lecture Notes in Earth Sciences, vol. 9. Springer-Verlag, New York, pp 183
24. Golubic, S, Seong-Joo, L, Browne, KM (2000) Cyanobacteria: architects of sedimentary structures. In: Riding, RE, Awramik, SM (Eds.) Microbial Sediments. Springer-Verlag, Berlin, Germany, pp 57–67
25. González-Toril, E, Llobet-Brossa, E, Casamayor, EO, Amann, R, Amils R (2003) Microbial ecology of an extreme acidic environment. The Tinto River. Appl Environ Microbiol 69: 4853–4865
26. Heinen, W, Lauwers, AM (1985) The microflora of radioactive thermal springs: the lithobionts in the Franz Joseph Springs at Badgastein Austria. Mikroscopic 42: 124–134
27. Hoagland, KD, Roemer, SC, Rosowski, R (1982) Colonization and community structure of two periphyton assemblages, with emphasis on the diatoms (Bacillariophyceae). Am J Bot 69(2): 188–213
28. Horodyski, R, Bloeser, J, Vonder Haar, S (1977) Laminated algal mats from a coastal lagoon Laguna Mormona, Baja California, Mexico. J Sediment Petrol 47: 680–696
29. Korte, VL, Blinn, DW (1983) Diatom colonization on artificial substrata in pool and riffle zones studied by light and scanning electron microscopy. J Phycol 19: 332–341
30. Langley, S, Beveridge, TJ (1999) Metal binding by *Pseudomonas aeruginosa* PA01 is influenced by growth of the cells as a biofilm. Can J Microbiol 45: 616–622
31. Lawrence, JR, Korber, DR, Hoyle, BD, Costerton, JW, Caldwell, D (1991) Optical sectioning of microbial biofilms. J Bacteriol 173: 6558–6567
32. López-Archilla, AI, Amils, R (1999) A comparative ecological study of two acidic rivers in southwestern Spain. Microb Ecol 38:146–156

33. López-Archilla, AI, Marín, I, Amils, R (2001) Microbial community composition and ecology of an acidic aquatic environment: the Tinto river, Spain. Microb Ecol 41: 20–35
34. López-Archilla, AI, Gonzalez, A, Terron, M, Amils, R (2004a) Ecological study of the fungal populations of the acidic Tinto River in southwestern Spain. Can J Microbiol 50: 923 – 934
35. Macfie, S, Tarmohamed, Y, Welbourn, PM (1994) Effects of cadmium, cobalt, copper, and nickel on growth of the green alga, *Chamydomonas reinhardtii*: the influences of the cell wall and pH. Arch Environ Contam Toxicol 27: 454 – 458
36. Nakatsu, C, Hutchinson, TC (1988) Extreme metal and acid tolerance of *Euglena mutabilis* and an associated yeast from Smoking Hills, Northwest Territories, and their apparent mutualism. Microb Ecol 16: 213 – 231
37. Nixdorf, B, Mischke, U, Lessmann, D (1998) Chrysophytes and Chlamydomonads: pioneer colonists in extremely acidic mining lakes (pH < 3) in Lusitania (Germany). Hydrobiologia 369–370: 315 – 327
38. Pedrozo, F, Kelly, L, Díaz, M, Temporetti, P, Baffico, G, Kringel, R, Friese, K, Mages, M, Geller, W, Woelfl, S (2001) First results on the water chemistry, algae and trophic status of an Andean acidic lake system of volcanic origin in Patagonia (Lake Caviahue). Hydrobiologia 452: 129 – 137
39. Peterson, R (1982) Influence of copper and zinc on the growth of a freshwater alga, *Scenedesmus quardicauda*: the significance of chemical speciation. Environ Sci Technol 16: 443 – 447
40. Pierson, BK, Parenteau, MN, Griffin, BM (1999) Phototrophs in high-iron-concentration microbial mats: physiological ecology of phototrophs in an iron-depositing hot spring. Appl Environ Microbiol 65: 5474 –5483
41. Seckbach, J, (1999) In: Seckbach, J, (Ed.) Enigmatic Microorganisms and Life in Extreme Environments. Kluwer Academic Publishers, pp 122
42. Sladeckova, A (1962) Limnological investigation methods for the periphyton community. Bot Rev 28: 286 –350
43. Sokal, RR, Rohlf, FJ (1981) Biometry. Freeman, San Francisco, CA, USA, pp 377
44. Stal, LJ, Défarge, C (2005) Structure and dynamics of exopolymers in an intertidal diatom biofilm. Geomicrobiol J 22: 341–352
45. Taylor, IS, Paterson, DM, Mehlert, A (1999) The quantitative variability and monosaccharide composition of sediment carbohydrates associated with intertidal diatom assemblages. Biogeochemistry 45: 303 –327
46. Tazaki, K, Rafiqul, I, Nagai, K, Kurihara, T (2003) $FeAs_2$ biomineralization on encrusted bacteria in hot springs: an ecological role of symbiotic bacteria. Can J Earth Sci 40: 1725 –1738
47. Tolker-Nielsen, T, Molin, S (2000) Spatial organization of microbial biofilm communities. Microb Ecol 40: 75 – 84
48. Van Hullebusch, ED, Zandvoort, MH, Lens, PNL (2003) Metal immobilisation by biofilms: mechanisms and analytical tools. Rev Environ Sci BioTechnol 2: 9 –33
49. Wierzchos, J, Ascaso, C (1994) Application of back-scattered electron imaging to the study of the lichen–rock interface. J Microsc 175: 54 –59
50. Wimpenny, J, Manz, W, Szewzyk, U (2000) Heterogeneity in biofilms. FEMS Microbiol Rev 24: 661– 671
51. Yamamoto, Y, Tatsuzawa, H, Wada, M (1998) Effect of environmental conditions on the composition of lipids and fatty acids on *Chlamydomonas* isolated from an acid lake. Verh Int Ver Limnol 26: 1788 –1790